Hindawi
International Transactions on Electrical Energy Systems
Volume 2023, Article ID 9804134, 1 page
https://doi.org/10.1155/2023/9804134

Retraction

Retracted: Application of the Lagrange Equation for Intelligent Sensor Vibration Control for Power Network Monitoring

International Transactions on Electrical Energy Systems

Received 19 September 2023; Accepted 19 September 2023; Published 20 September 2023

This article has been retracted by Hindawi following an investigation undertaken by the publisher [1]. This investigation has uncovered evidence of one or more of the following indicators of systematic manipulation of the publication process:

(1) Discrepancies in scope

(2) Discrepancies in the description of the research reported

(3) Discrepancies between the availability of data and the research described

(4) Inappropriate citations

(5) Incoherent, meaningless and/or irrelevant content included in the article

(6) Peer-review manipulation

The presence of these indicators undermines our confidence in the integrity of the article's content and we cannot, therefore, vouch for its reliability. Please note that this notice is intended solely to alert readers that the content of this article is unreliable. We have not investigated whether authors were aware of or involved in the systematic manipulation of the publication process.

Wiley and Hindawi regrets that the usual quality checks did not identify these issues before publication and have since put additional measures in place to safeguard research integrity.

We wish to credit our own Research Integrity and Research Publishing teams and anonymous and named external researchers and research integrity experts for contributing to this investigation.

The corresponding author, as the representative of all authors, has been given the opportunity to register their agreement or disagreement to this retraction. We have kept a record of any response received.

References

[1] X. Cheng, "Application of the Lagrange Equation for Intelligent Sensor Vibration Control for Power Network Monitoring," *International Transactions on Electrical Energy Systems*, vol. 2022, Article ID 4616889, 9 pages, 2022.

Hindawi
International Transactions on Electrical Energy Systems
Volume 2022, Article ID 4616889, 9 pages
https://doi.org/10.1155/2022/4616889

Research Article

Application of the Lagrange Equation for Intelligent Sensor Vibration Control for Power Network Monitoring

Xiaojing Cheng

School of Mathematics and Computer Science, Shaanxi University of Technology, Hanzhong 723001, Shaanxi, China

Correspondence should be addressed to Xiaojing Cheng; 20141296@stu.sicau.edu.cn

Received 14 July 2022; Revised 26 August 2022; Accepted 5 September 2022; Published 29 September 2022

Academic Editor: Nagamalai Vasimalai

Objective. In order to control the vibration of the beam structure more effectively and improve the safety and availability of the beam structure, an application study of the Lagrange equation for vibration control of smart sensors for power grid monitoring is proposed. The vibration of the beam structure, the displacement of the beam structure under the excitation of seismic acceleration, the response analytical electrical formula, and the displacement response formula of the beam structure under the action of the kinematic force are deduced. The optimal parameters of the beam-TMDI system are given, and the parameter sensitivity analysis is carried out. Then, the control effect of the TMDI system is studied by numerical analysis, and the vibration reduction effect of the TMDI system and the tuned mass damper (TMD) system is compared. Experimental results show that when the mass ratio μ of the TMDI system and the TMD system are both set to a fixed value of 0.005, and the parameter β of the TMDI system is set to 0, namely $\beta = b = 0$, at this time, the TMDI system degenerates into a TMD system. The TMD natural frequency is 14.179 rad/s and the damping ratio is 0.0432 by the DH optimization method, while the TMD natural frequency is 14.1812 rad/s, and the damping ratio is 0.0436 by the augmented Lagrangian optimization algorithm. *Conclusion*. The vibration displacement response spectrum of a beam structure obtained by the frequency domain method can effectively reflect electricity in the displacement response of a beam structure. The parameters that minimize the vibration response of the beam structure can be accurately obtained by using the augmented Lagrangian parameter optimization method. The sensitivity of the TMDI system is controlled by the inertial device, and the inertial device has a significant impact on its robustness. The vibration reduction performance of the TMDI system is obviously better than in the conventional TMD systems.

1. Introduction

With the rapid economic development and the continuous progress of science and technology in various countries in the world, the structural systems of high-rise buildings are also constantly developing. The continuous development of concrete and steel has promoted electricity and the diversity and rationality of building structural systems, from the multistorey frame structure system to the emergence of high-rise and super high-rise buildings, which all reflect the perfect combination of social needs and technological progress in electricity. High-rise and super high-rise structures are moving towards a more integrated and intelligent direction. In the late 1960s, with the continuous development and improvement of the lateral force resistance system, the height of high-rise buildings continued to increase. A super high-rise building structural system evolved from the beam-type transfer storey structure and giant building structural system came into being [1].

My country is in the most active seismic zone and is one of the most earthquake-prone countries. Earthquake disasters have two characteristics: suddenness and destructiveness. Previous earthquake disasters have caused incalculable loss of life and property in my country [2]. Research on the vibration control of building structural systems, combining the unique two-level structure of giant structures with structural vibration control technology, and the emergence of a new type of giant vibration reduction system, can not only reduce the impact of earthquake damage but also solve the problem of difficult earthquake

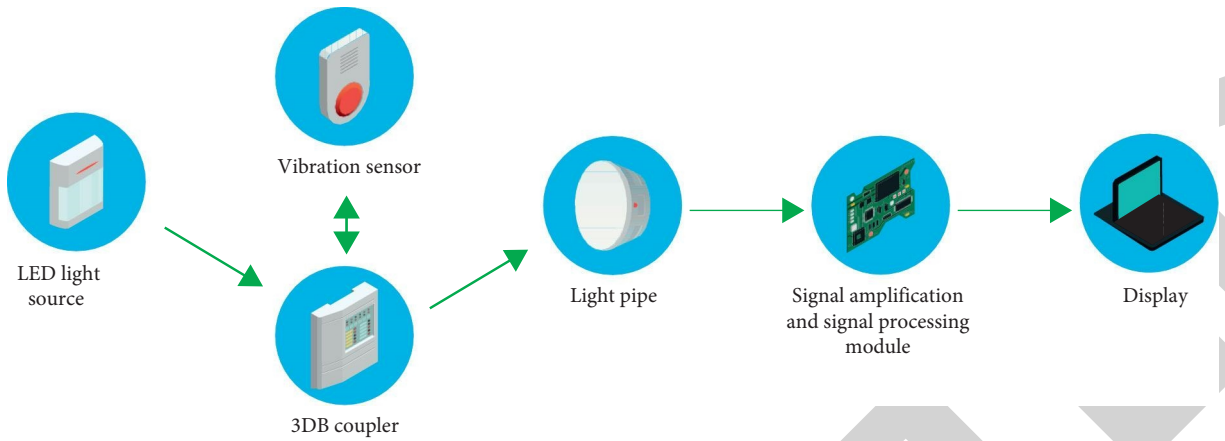

Figure 1: The intelligent sensor of the Lagrange dynamics equation.

resistance of high-rise structures to a certain extent, which is of great significance for engineering earthquake resistance [3].

Engineering structure vibration reduction control technology refers to the addition of control devices (or a certain mechanism, substructure, and external force) to some parts of the engineering structure, such as vibration isolation bearings, tuning mass blocks, energy dissipation supports, and others, used to change or adjust the dynamic parameters of the structure. The structural response of the structural system under the action of an earthquake or wind load is controlled within a certain range in order to ensure the safety and normal use of the structure. The related theories, technologies, and methods are collectively referred to as "engineering structure vibration reduction control", as shown in Figure 1.

2. Literature Review

Refani et al. studied an L-shaped composite beam structure, considered the nonlinear models of the in-plane vibration and out-of-plane vibration of the L-shaped composite beam structure, and derived all nonlinear motion equations, including second-order nonlinearity [4]. Khosravi et al. studied the natural frequency and global mode shape of the L-shaped composite beam structure and obtained them by the global modal method and compared with the results calculated by the finite element method. The effectiveness of this method for solving L-shaped composite beams is illustrated [5]. Chen et al. used the global modal method to study the U-shaped composite beam structure, obtained the frequency equation of the U-shaped beam structure, and obtained the natural frequency and global mode of the system [6]. Ebrahimi-Mamaghani derived the governing equations of the plane motion of the Z-shaped composite beam structure and the boundary conditions of the system by using the Hamilton's principle and theoretically obtained the natural frequency of the Z-shaped composite beam structure and the modal mode shape of the analytical form [7]. Tk et al. considered the bending and torsional deformation of the rod and the bending deformation of the beam. The bending and torsional motion of the T-beam were dynamically modeled by using the global modal idea, and the characteristic equations and dynamic equations of the system were obtained [8]. Kheiri used piezoelectric sheets to control the bending vibration of the beam and used piezoelectric rings to control the torsional vibration of the rod and obtained a good control effect [9]. Chen et al. fixed active vibration control of beam structures at one end and stressed at one end by piezoelectric actuators. Based on the Euler–Bernoulli beam theory, the governing equations of the system are derived [10]. Wei et al. concluded that based on the robust control method, the vibration control problem of a piezoelectric smart beam structure was analyzed [11].

Therefore, the author proposes to use the TMDI system to control the vibration electricity of the beam structure under the action of seismic acceleration and moving force, respectively. Firstly, the mechanical analysis model under the action of seismic acceleration and moving force is established; secondly, the combination of the virtual excitation method and the Fourier transform method is used. The displacement response spectrum of the beam structure under seismic acceleration excitation is deduced, and the vibration displacement response spectrum of the beam structure under moving load is deduced by the Fourier transform. Then, on this basis, the TMDI optimal parameters that minimize the vibration response of the beam structure are obtained by using the augmented Lagrangian optimization algorithm. Finally, through an example analysis, the sensitivity of the optimal parameters of the TMDI system under the action of seismic acceleration and moving load of the beam structure in the frequency domain, the influence of the inertial device on the robustness of the TMDI system, as well as the superiority of the TMDI system are compared to the TMD system.

3. Research Methods

3.1. Frequency Domain Response of Beam-TMDI System under Random Load Excitation

3.1.1. Vibration under Seismic Acceleration. For a simply supported beam with a span of L, and a TMDI vibration reduction system is set in the middle of the span, the motion

equation of the beam-TMDI system under the excitation of seismic acceleration $\ddot{x}_g(t)$ can be expressed as in the following equations:

$$[M]\{\ddot{y}\} + [C]\{\dot{y}\} + [K]\{y\} = -[M][E]\ddot{x}_g(t) + F_T, \quad (1)$$

$$F_T = D_d[c_d(\dot{x}_d - \dot{y}) + k_d(x_d - y)], \quad (2)$$

$$(b + m_d)\ddot{x}_d + c_d(x_d - \dot{y}) + k_d(x_d - y) = -m_d\ddot{x}_g(t). \quad (3)$$

Here, $[M]$ is the mass matrix; $[C]$ is the damping matrix; $[K]$ is the stiffness matrix; $E = [1, 1, \cdots, 1]$; $\{y\}$ is the displacement of the beam structure relative to the ground, namely $\{y\} = \{y_1, y_2, \cdots, y_j\}^T$; F_T is the reaction force of the TMDI system to the simply supported beam; m_d, k_d, c_d, and b are the mass parameters of TMDI, spring stiffness, damping, and inertial mass parameters, respectively; x_d is the vertical displacement of the mass block of the TMDI system; and $D_d = [0, \ldots, 0, 1, 0, \ldots, 0]$ [12, 13]. Using the mode shape decomposition method of the structural equation of motion, the vertical displacement $y(x,t)$ of a simply supported beam at a time x and position t can be expressed as a linear combination of beam mode shapes, that is shown in the following formula:

$$y(x,t) = \sum_{j=1}^{q} u_j(t)\phi_j(x), \quad (4)$$

where $\phi_j(x)$ is the first mode shape of the beam, and for a simply supported beam of equal section, the mode shape function is $\phi_j(x) = \sin(j\pi x/L)$; $u_j(t)$ is the generalized coordinate corresponding to the j-th mode of the simply supported beam [13]. The virtual acceleration excitation is constructed using the known self-spectrum as follows:

$$\ddot{\tilde{x}}_g(t) = \sqrt{S_{\ddot{x}_g}(\omega)}e^{i\omega t}. \quad (5)$$

Multiplying equation (1) on the left by $[\phi]^T$, then substituting equations (4) and (5) into equation (1) and using the orthogonality of mode shapes, the following equation can be obtained:

$$[\overline{M}]\{\ddot{\tilde{u}}\} + [\overline{C}]\{\dot{\tilde{u}}\} + [\overline{K}]\{\tilde{u}\} = -[\phi]^T[M][E]\sqrt{S_{\ddot{x}_g}(\omega)}e^{i\omega t} + [\phi]^T F_T. \quad (6)$$

In the formula, the symbol ~ is a virtual quantity; $[\overline{M}] = [\phi]^T[M][\phi]$; $[\overline{C}] = [\phi]^T[C][\phi]$; $[\overline{K}] = [\phi]^T[K][\phi]$; F_T is the reaction force of the TMDI system to the simply supported beam; then equation (6) is decomposed into mutually independent single degree-of-freedom equations, as shown in the following equation:

$$\ddot{\tilde{u}}_j + 2\xi_j\omega_j\dot{\tilde{u}}_j + \omega_j^2\tilde{u}_j = -\gamma_j\sqrt{S_{\ddot{x}_g}(\omega)}e^{i\omega t} + \frac{\phi_j(L/2)}{m_j}\left\{c_d\left(\dot{x}_d - \phi_j\left(\frac{L}{2}\right)\dot{\tilde{u}}_j\right) + k_d\left(x_d - \phi_j\left(\frac{L}{2}\right)\tilde{u}_j\right)\right\}. \quad (7)$$

Here, ω_j, ξ_j, and m_j are the jth-order frequency, damping ratio, and mode mass of the structure, respectively; $\gamma_j = [\phi]^T[M][E]/[\phi]^T[M][\phi]$. For the convenience of calculation, the parameter $\alpha_j = m_d\phi_j(L/2)/m_j$, $v_s = x_d - \phi_j(L/2)\tilde{u}_j, \dot{v}_s = \dot{x}_d - \phi_j(L/2)\dot{\tilde{u}}_j$ is defined.

Formula (7) can be simplified to the following formula:

$$\ddot{\tilde{u}}_j + 2\xi_j\omega_j\dot{\tilde{u}}_j + \omega_j^2\tilde{u}_j = -\gamma_j\sqrt{S_{\ddot{x}_g}(\omega)}\,e^{i\omega t} + \alpha_j\left(2\xi_d\omega_d\dot{v}_s + \omega_d^2 v_s\right), \quad (8)$$

where ω_d is the frequency of the TMDI damper; $\xi_d = c_d/2m_d\omega_d$ is the damping ratio of the TMDI damper [14]. Assuming $b/m_d = \Theta$, the equation of motion (3) of TMDI can be further simplified as follows:

$$(\Theta + 1)\ddot{x}_d + \ddot{x}_g + 2\omega_d\xi_d\dot{v}_s + \omega_d^2 v_s = 0. \quad (9)$$

Simultaneously formula (8) and formula (9) can be written in the matrix form as follows:

$$\widehat{M}_j\ddot{\tilde{y}}_j + \widehat{C}_j\dot{\tilde{y}}_j + \widehat{K}_j\tilde{y}_j = \widehat{F}_j. \quad (10)$$

In the formula, $\tilde{y}_j = [\tilde{u}_j, v_s]^T$; $\widehat{F}_j = [-\gamma_j\sqrt{S_{\ddot{x}_g}(\omega)}\,e^{i\omega t}, -\ddot{\tilde{x}}_g]^T$;

$$\widehat{M}_j = \begin{bmatrix} 1 & 0 \\ (\Theta+1)\phi_j(L/2) & \Theta+1 \end{bmatrix}; \widehat{K}_j = \begin{bmatrix} \omega_j^2 & -\alpha_j\omega_d^2 \\ 0 & \omega_d^2 \end{bmatrix};$$

$$\widehat{C}_j\begin{bmatrix} 2\xi_j\omega_j & -2\alpha_j\xi_d\omega_d \\ 0 & 2\omega_d\xi_d \end{bmatrix}.$$

Perform the Fourier transform on equation (10) to get the following equation:

$$\tilde{Y}_j(\omega) = \left(-\omega^2\widehat{M}_j + i\omega\widehat{C}_j + \widehat{K}_j\right)^{-1}\tilde{F}_j(\omega). \quad (11)$$

Equation (11) can also be written as

$$\begin{Bmatrix} \tilde{u}_j(\omega) \\ v_s \end{Bmatrix} = \begin{bmatrix} H_j(\omega) & H_{js}(\omega) \\ H_{sj}(\omega) & H_s(\omega) \end{bmatrix}\begin{Bmatrix} -\gamma_j\sqrt{S_{\ddot{x}_g}(\omega)} \\ -\sqrt{S_{\ddot{x}_g}(\omega)} \end{Bmatrix}. \quad (12)$$

Then, the jth-order modal response component of the simply supported beam is shown in the following equation:

$$\widetilde{u}_j(\omega) = -H_j(\omega)\gamma_j\sqrt{S_{\ddot{x}_g}(\omega)} - H_{jj}(\omega)\sqrt{S_{\ddot{x}_g}(\omega)} = H(\omega)\cdot\sqrt{S_{\overline{x}_g}(\omega)}. \tag{13}$$

In the following formula, the transfer function $H(\omega)$ is expressed as

$$H(\omega) = \frac{-\gamma_j - \left(i\omega 2\alpha_j\xi_d\omega_d + \alpha_j\omega_d^2\right)X^{-1}}{-\omega^2 + i\omega 2\xi_j\omega_j + \omega_j^2 - X^{-1}\omega^2(\Theta+1)\phi_j(L/2)\left(i\omega 2\alpha_j\xi_d\omega_d + \alpha_j\omega_d^2\right)}. \tag{14}$$

In the formula, $X = -\omega^2(\Theta+1) + i\omega 2\xi_d\omega_d + \omega_d^2$. Then, the displacement response spectrum of the simply supported beam in the frequency domain under seismic acceleration excitation is given in the following formula:

$$\widetilde{Y}(\omega) = \sum_{j=1}^{q}\widetilde{u}_j(\omega)\phi_j(x) = \sum_{i=1}^{q}H(\omega)\phi_j(x)\sqrt{S_{\overline{x}_g}(\omega)}. \tag{15}$$

For the first-order mode shape of the simply supported beam, the mid-span vibration displacement response spectrum $\widetilde{Y}_1(\omega)$ of the simply supported beam considering the TMDI system under seismic acceleration excitation is given in the following formula:

$$\widetilde{Y}_1(\omega) = \frac{-\gamma_1 - \left[m_d\phi_1(L/2)/m_1\xi_d\omega_d + m_d\phi_1(L/2)/m_1\omega_d^2\right]X^{-1}\cdot\phi_1(L/2)\cdot\sqrt{S_{\overline{x}_g}(\omega)}}{-\omega^2 + i\omega 2\xi_1\omega_1 + \omega_1^2 - X^{-1}\omega^2\left(b/m_d{+}1\right)\phi_1(L/2)\left[m_d\phi_1(L/2)/m_1\xi_d\omega_d + m_d\phi_1(L/2)/m_1\omega_d^2\right]}. \tag{16}$$

$$\ddot{u}_j(t) + 2\xi_j\omega_j\dot{u}_j(t) + \omega_j^2u_j(t) = \left[F_{bj}(t) + F_{Tj}(t)\right], \tag{17}$$

3.1.2. Vibration under Moving Loads. When the vibration response of a simply supported beam under the excitation of a moving load is controlled by TMDI, it is assumed that the moving concentrated force p_0 moves at a uniform velocity v on the simply supported beam with a span, and the equation of motion of a standard single degree-of-freedom system with mode shape coordinates as variables is established, it is shown in the following formula:

where, $u_j(t)$ is the generalized coordinate corresponding to the j-th mode of the simply supported beam; $F_{bj}(t)$ is the j-th mode load of the moving concentrated force; and $F_{Tj}(t)$ is the j-th mode force of the TMDI, and the expressions are as follows:

$$F_{bj}(t) = \frac{1}{m_j}p_0\sin\frac{j\pi vt}{L}, \tag{18}$$

$$\begin{aligned} F_{Tj}(t) &= \frac{1}{m_j}\phi_j\left(\frac{L}{2}\right)\left\{k_d\left[x_d - \phi_j\left(\frac{L}{2}\right)u_j(t)\right] + c_d\left[\dot{x}_d - \phi_j(L/2)\dot{u}_j(t)\right]\right\}, \\ &= \frac{m_d}{m_j}\phi_j(L/2)\left\{\omega_d^2\left[x_d - \phi_j(L/2)u_j(t)\right] + 2\zeta_d\omega_d\left[\dot{x}_d - \phi_j(L/2)\dot{u}_j(t)\right]\right\}. \end{aligned} \tag{19}$$

For the convenience of calculation, the following parameters are defined:

$$\alpha_j = \phi_j\left(\frac{L}{2}\right)\frac{m_d}{m_j}, \varepsilon_j = \frac{b}{m_j},$$

$$v_j = x_d - \phi_j\left(\frac{L}{2}\right)u_j(t), \dot{v}_j = \dot{x}_d - \phi_j\left(\frac{L}{2}\right)\dot{u}_j(t), (t), \tag{20}$$

$$\ddot{v}_j = \ddot{x}_d - \phi_j\left(\frac{L}{2}\right)\ddot{u}_{j.}$$

Formula (19) can be simplified to the following formula:

$$F_{Tj}(t) = \alpha_j\left(\omega_d^2 v_j + 2\xi_d\omega_d\dot{v}_j\right). \tag{21}$$

And because of $F_{Tj}(t) = -\phi_j(L/2)(m_d + b)\ddot{x}_d/m_j$, the following formula can be deduced.

$$\varepsilon_j\left[\ddot{v}_j + \phi_j(L/2)\ddot{u}_j\right] + \omega_d^2 v_j + 2\xi_d\omega_d\dot{v}_j = 0. \tag{22}$$

Simultaneously from formula (19), formula (21), and formula (22), the equation system is written in the matrix form as shown in the following formula:

$$\hat{M}_j\ddot{y}_j + \hat{C}_j\dot{y}_j + \hat{K}_j y_j = \hat{F}_j. \tag{23}$$

Fourier transform is performed on the above equation to obtain equation

$$\mathrm{Y_j}(\omega) = \left(-\omega^2\hat{\mathrm{M}}_\mathrm{j} + i\omega\hat{\mathrm{C}}_\mathrm{j} + \hat{\mathrm{K}}_\mathrm{j}\right)^{-1}\hat{\mathrm{F}}_\mathrm{j}(\omega). \tag{24}$$

Then, the jth-order modal response of the simply supported beam is

$$u_j(\omega) = H_j(\omega)F_{bj}(\omega). \tag{25}$$

The expression of the transfer function $H_j(\omega)$ is the following formula:

$$H_j(\omega) = \left[-\omega^2 + 2i\omega\xi_j\omega_j + \omega_j^2 - \omega^2\varepsilon_j\phi_j(L/2)X^{-1}\left(2\xi_d\omega_d i\omega + \alpha_j\omega_d^2\right)^{-1}\right], \tag{26}$$

where $X = -\omega^2\varepsilon_j + 2\xi_d\omega_d i\omega + \omega_d^2$; $F_{bj}(\omega)$ is the Fourier transform of the j-th mode load; and $F_{bj}(t)$ of the moving concentrated force, which is given in the following formula:

$$F_{bj}(\omega) = \frac{1}{m_j}p_0\frac{j\pi v/L}{\omega^2 - (j\pi v/L)^2}\left[(-1)^j e^{-i\omega(L/v)} - 1\right]. \tag{27}$$

Then, the vibration displacement response spectrum $Y(\omega)$ of the simply supported beam under the excitation of the moving force is as follows:

$$Y(\omega) = H_j(\omega)\cdot F_{bj}(\omega)\cdot\phi_j(x). \tag{28}$$

For the first mode shape of the simply supported beam, the mid-span vibration displacement response spectrum $Y_1(\omega)$ of the simply supported beam with the TMDI system set up under the moving load excitation is given in the following formula:

$$Y_1(\omega) = \frac{1/m_1 p_0\left[(-2\pi L/v) - (\pi)^2\right]^{-1}\cdot\cos(\omega L/2v)\cdot e^{-1(\omega L/2v)}\cdot\phi_1(L/2)}{-\omega^2 + i\omega 2\xi_1\omega_1 + \omega_1^2 - \omega^2(b/m_d)\phi_1(L/2)X^{-1}\left[2\xi_d\omega_d i\omega + \phi_1(L/2)\cdot m_d/m_1\omega_d^2\right]}. \tag{29}$$

3.2. Optimal TMDI System. In order to minimize the vibration response of a simply supported beam, the parameters of the TMDI must be optimized. For the convenience of calculation, define two parameters μ and β, where $\mu = m_d/m_1$ is the ratio of the TMDI mass m_d to the first-order mode mass m_1 of the simply supported beam. $\beta = b/m_1$ is the mass parameter b of the inertial device, and the first-order of the simply supported beam, is the ratio of mode shape to mass m_1 [15]. In the present study, the parameters of TMDI are μ, β, ω_d, and ξ_d where ξ_d is the natural circular frequency and damping ratio of the TMDI system, respectively [16].

The design of the optimal TMDI parameters includes two steps: first, select the appropriate mass ratio$\mu$and β. Second, find the optimal ω_d and ξ_d based on μ and β. In order to obtain the optimal ω_d and ξ_d, the author proposes to

Table 1: Simply supported beam parameters.

Parameter	Beam length L/m	Bending stiffness of section $EI/(N \cdot m^2)$	Mass per unit length $m/(kg \cdot m^{-1})$	Damping ratio ξ_1	First-order natural frequency $\omega_1/(rad \cdot s^{-1})$
Numerical value	20	1×109	3000	0.025	14.25

use the augmented Lagrange multiplier method for analysis. The augmented Lagrangian multiplier method is a method combining the penalty function outlier method on the basis of the Lagrangian multiplier method [17]. The author adopts the method of MATLAB programming to realize the purpose of finding the optimal parameters.

3.2.1. Optimization of Beam-TMDI System under Seismic Acceleration Excitation

$$\min \tilde{y}(\omega) = H_1(\omega) \cdot \phi_1(x) \cdot \sqrt{S_{\ddot{x}_g}(\omega)}, \tag{30}$$

$$s.t.\ h(\omega) = \max \tilde{y}_1(\omega) - \max \tilde{y}_2(\omega) = 0. \tag{31}$$

In formulas (30) and (31), $H_1(\omega)$ is the frequency response function; $h(\omega)$ is the constraint condition;

$\max \overline{y}_1(\omega)$ is the maximum value of $\overline{y}_1(\omega)$ in the interval $0, \omega_1$; $\max \overline{y}_2(\omega)$ is the maximum value of $\overline{y}_2(\omega)$; and ω_0 is a certain frequency value and $\omega_0 > \omega_1$

The augmented Lagrangian function of the optimization problem is shown in the following formula:

$$L(\omega, \lambda, \delta) = \tilde{y}(\omega) + \lambda h(\omega) + \frac{\delta}{2} h^2(\omega), \tag{32}$$

where λ is the initial Lagrange multiplier and δ is the positive penalty coefficient.

3.2.2. Optimization of Beam-TMDI System for Moving Force Excitation

$$\min y(\omega) = H_1(\omega) \cdot \phi_1(x) \cdot F_{b1}(\omega), \tag{33}$$

$$s.t.\ h(\omega) = \max y_1(\omega) - \max y_2(\omega) = 0, \tag{34}$$

$$L(\omega, \lambda, \delta) = y(\omega) + \lambda h(\omega) + \frac{\delta}{2} h^2(\omega). \tag{35}$$

In formulas (33)–(35), $\max y_1(\omega)$ is the maximum value of $y_1(\omega)$ in the interval $(0, \omega_1)$; $\max y_2(\omega)$ is the maximum value of $y_2(\omega)$ in the interval (ω_1, ω_0).

4. Analysis of Results

Taking a simply supported beam as an example, the effectiveness of the TMDI control system under two different types of loads is studied. The parameters of the beam are shown in Table 1. The seismic acceleration spectrum adopts the Kanai–Tajimi spectrum, and its parameters are $\omega_g = 15.54 rad/s$, $\xi_g = 0.8523$, and $S_0 = 0.0143$. The magnitude of the moving force and the moving speed are $p_0 = 6000kN$ and $v = 60m/s$, respectively.

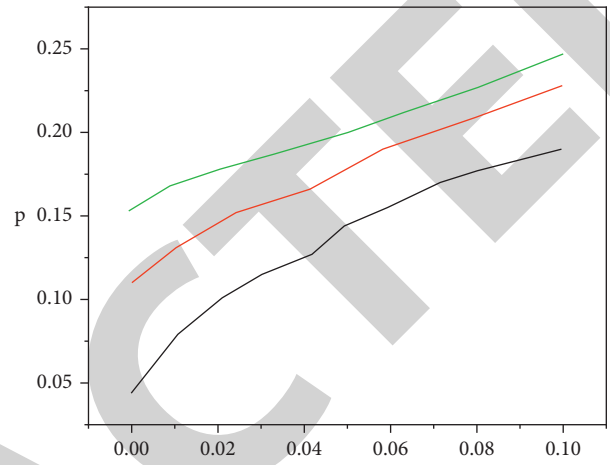

Figure 2: The influence of mass ratios μ and β on the optimal damping ratio of TMDI.

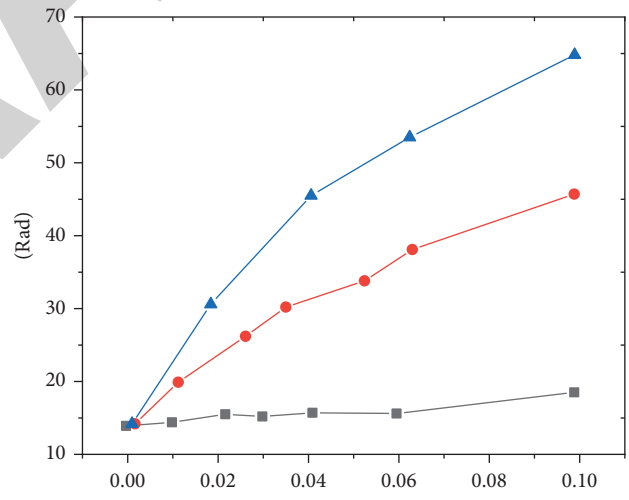

Figure 3: The influence of mass ratios μ and β on the optimal frequency of TMDI.

4.1. Optimal TMDI Parameters. Similar to the traditional tuned mass damper TMD, in order to optimize the damping performance of the TMDI system, parameter optimization must be carried out [18]. For different mass ratios μ and parameters β, the authors used the augmented Lagrangian optimization algorithm to optimize the TMDI damping ratio ξ_d and frequency ω_d, the optimal damping ratio ξ_d and the optimal frequency ω_d, respectively, as shown in Figures 2 and 3. As the mass ratio increases, the optimal damping ratio ξ_d of the TMDI system also increases, while the optimal frequency ω_d decreases [19]. At present, the inertial device of TMDI can amplify the physical mass of the damper by 60

times to 200 times through the setting of the parameter β [20].

It is worth noting that the TMDI system has different characteristics from the traditional TMD system. The optimal frequency of the traditional TMD system is close to the first-order natural frequency of the structure, while the optimal natural circular frequency ω_d of the TMDI system obtained by the author is much larger than the first-order natural frequency of the structure. For example, when the mass ratios are $\mu = 0.005$ and $\beta = 0.03$, the optimal damping ratio and natural circle frequency of the TMDI damper obtained by the augmented Lagrangian optimization algorithm are $\xi_d = 0.1154$ and $\omega_d = 37.5199 rad/s$, respectively. The first-order natural circular frequency of the known structure is $\omega_1 = 14.25 rad/s$, and it is obvious that ω_d is much larger than ω_1. The optimal TMDI frequency values obtained by many scholars have similar characteristics.

4.2. Parameter Sensitivity Analysis. When the TMDI system adopts the optimal frequency and damping ratio, its vibration reduction performance is optimal, and the acquisition of these parameters is only related to the characteristics of the structure itself. But there are some uncertain factors in the actual structure, so it is necessary to carry out the robustness analysis of the TMDI system. Due to space limitations, the effect of the variation of design parameters ω_d and ξ_d on the maximum displacement response of the beam-TMDI system for different mass ratios μ and β under the action of moving force is shown [21]. The 3D surface exhibits a long and narrow shape, which means that the disturbance has a significant effect on the control performance. Changing the TMDI frequency can significantly change the control effect, while changing the TMDI damping ratio has little effect on the system control performance. In other words, the beam-TMDI system control performance is more sensitive to frequency. When the mass ratio μ increases, the variation range of the maximum displacement response is smaller, which indicates that the robustness of the system is stronger when the μ value increases, which is consistent with the TMD system ($\beta = 0$). In addition, when the mass ratio μ is the same, the width of the concave surface becomes wider as the β value becomes larger [22].

4.3. Simply Supported Beams—Effectiveness of the TMDI System. In order to study whether the simply supported beam is excited by seismic acceleration and moving force, whether installing the TMDI system at the mid-span position can effectively control the vibration response of the beam structure, first, set the mass ratio μ of the TMDI system to a certain value of 0.005, and β to 0.01, 0.03, and 0.05, respectively. Then, the optimal parameters of the TMDI system are obtained by the augmented Lagrangian optimization algorithm, and the frequency domain response analysis of the simply supported beam structure under seismic acceleration and moving force excitation is carried out. In addition, when the mass ratio μ is constant and as the mass ratio β increases, the control effect of the TMDI system is better. Therefore, installing a TMDI system in the mid-span of a simply supported beam can significantly reduce its displacement response [23].

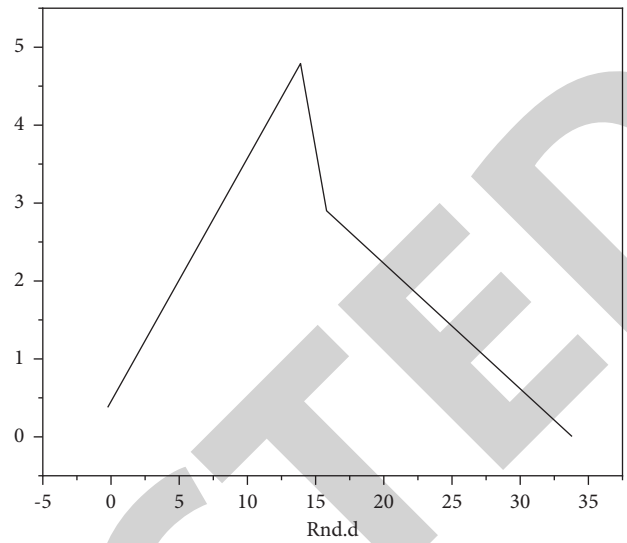

Figure 4: Comparison of vibration reduction performances of TMDI and TMD systems under seismic acceleration.

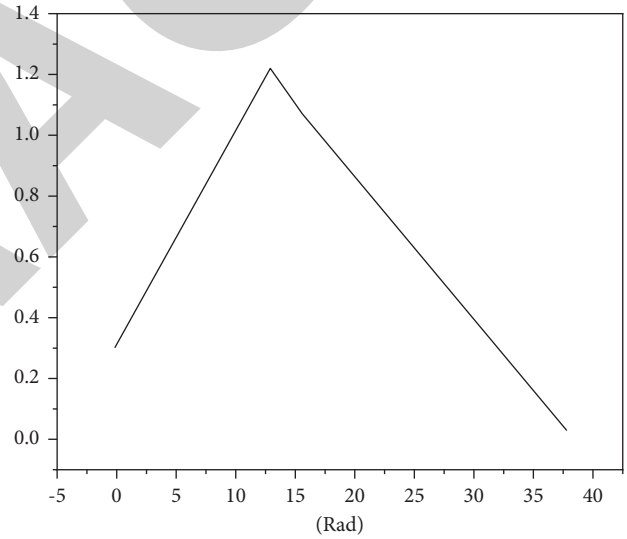

Figure 5: Comparison of vibration reduction performances of TMDI and TMD systems under moving force.

4.4. Performance Comparison of TMDI and TMD Systems. In order to effectively carry out comparative analysis, the mass ratio μ of the TMDI system and the TMD system is set to a fixed value of 0.005, and the parameter β of the TMDI system is set to 0, that is, $\beta = b = 0$, at this time, the TMDI system degenerates into a TMD system. The vibration reduction effects of the optimal TMD parameters obtained by these two optimization methods are shown in Figures 4 and 5, which are in complete agreement. This also verifies the correctness of the augmented Lagrangian optimization algorithm [24].

In order to further analyze the superiority of the TMDI system, the parameter β is set to 0.03. After parameter optimization based on the augmented Lagrangian optimization algorithm, the displacement responses in the frequency domain under the action of seismic acceleration and moving force, respectively, are obtained, as shown in Figure 4 and shown in the solid line part of Figure 5. The vibration reduction performance of the TMDI system is obviously better than that of the TMD system.

5. Conclusion

Based on the analysis results, the following conclusions are drawn:

(1) When the mass ratio remains unchanged, the vibration reduction performance electricity of the beam-TMDI system increases with the increase in the mass ratio.

(2) The vibration reduction performance of the TMDI system is more sensitive to the TMDI frequency value, while the damping ratio has less influence on its control effect.

(3) When the mass ratio is small, the robustness of the TMDI system is mainly controlled by the inertial device, and the inertial device has an obvious influence on its robustness.

(4) When using TMDI to control the vibration response electricity of the simply supported beam structure under the excitation of seismic acceleration and moving force, its vibration reduction effect is obviously better than that of the simply supported beam structure under TMD control, especially when the mass ratio is smaller than μ.

Data Availability

The data used to support the findings of this study are available from the author upon request.

Conflicts of Interest

The author declares no conflicts of interest.

Acknowledgments

The study was supported by Foundation of "Shaanxi Educational of Committee," under Project No. 11JK0514.

References

[1] A. Taale, C. E. Ventura, and J. Marti, "On the feasibility of iot-based smart meters for earthquake early warning," *Earthquake Spectra*, vol. 37, no. 3, pp. 2066–2083, 2021.

[2] T. Kishida, D. S. Park, R. L. Sousa, R. Armstrong, and Y. J. Byon, "Modulus reductions of dam embankment materials based on downhole array time series," *Earthquake Spectra*, vol. 36, no. 1, pp. 400–421, 2020.

[3] G. Lanzano and L. Luzi, "A ground motion model for volcanic areas in Italy," *Bulletin of Earthquake Engineering*, vol. 18, no. 1, pp. 57–76, 2020.

[4] A. N. Refani, Y. Tajunnisa, K. Yudoprasetyo, F. Ghifari, and D. I. Wahyudi, "Evaluation of structure performance under seismic load with non-liner time history on high-rise building affected by kendeng fault earthquake simulation," *Key Engineering Materials*, vol. 879, pp. 232–242, 2021.

[5] F. Khosravi, S. A. Hosseini, and A. Tounsi, "Forced axial vibration of a single-walled carbon nanotube embedded in elastic medium under various moving forces," *Journal of Nano Research*, vol. 63, pp. 112–133, 2020.

[6] H. Y. Chen, H. Ding, S. H. Li, and L. Q. Chen, "The scheme to determine the convergence term of the galerkin method for dynamic analysis of sandwich plates on nonlinear foundations," *Acta Mechanica Solida Sinica*, vol. 34, no. 1, pp. 1–11, 2021.

[7] A. Ebrahimi-Mamaghani, A. Hs, and B. Mr, "On the vibrations of axially graded Rayleigh beams under a moving load," *Applied Mathematical Modelling*, vol. 84, pp. 554–570, 2020.

[8] A. Tk, A. Ab, and A. Rk, "Optimization of multilayer rail substrate under moving load, using metamaterials," *Procedia Computer Science*, vol. 176, pp. 3399–3406, 2020.

[9] F. Kheiri, "A multistage recursive approach in time- and frequency-domain for thermal analysis of thermochromic glazing and thermostatic control systems in buildings," *Solar Energy*, vol. 208, pp. 814–829, 2020.

[10] Y. Chen, J. Xu, Y. Gao, L. Lin, J. Cao, and H. Ma, "Analysis and design of phase-shift pulse-frequency-modulated full-bridge LCC resonant converter," *IEEE Transactions on Industrial Electronics*, vol. 67, no. 2, pp. 1092–1102, 2020.

[11] Y. Wei, Q. Luo, and A. Mantooth, "Comprehensive comparisons between frequency-domain analysis and time-domain analysis for LLC resonant converter," *IET Power Electronics*, vol. 13, no. 9, pp. 1735–1745, 2020.

[12] T. Chen, Y. Zhu, X. X. Xi, H. Huan, and W. Ding, "Process parameter optimization and surface integrity evolution in the high-speed grinding of tial intermetallics based on grey relational analysis method," *International Journal of Advanced Manufacturing Technology*, vol. 117, no. 9-10, pp. 2895–2908, 2021.

[13] K. Nagai, K. Nagato, T. Osa et al., "Parameter optimization in the drying process of catalyst ink for pefc electrode films with few cracks," *ECS Transactions*, vol. 104, no. 9, pp. 17–23, 2021.

[14] X. Chen, X. Gao, X. Lin, J. Liu, and L. Le, "A novel method for rapidly calculating explosion dynamic displacement response of reticulated shell structure based on influence surfaces," *Advances in Structural Engineering*, vol. 23, no. 6, pp. 1098–1113, 2020.

[15] Y. R. Lee, H. S. Kim, and J. W. Kang, "Seismic response control performance evaluation of tuned mass dampers for a retractable-roof spatial structure," *International Journal of Steel Structures*, vol. 21, no. 1, pp. 213–224, 2021.

[16] W. H. Xu, Q. N. Zhang, W. C. Ma, and E. H. Wang, "Response of two unequal-diameter flexible cylinders in a side-by-side arrangement: characteristics of fiv," *China Ocean Engineering*, vol. 34, no. 4, pp. 475–487, 2020.

[17] P. S. Phani and W. C. Oliver, "Critical examination of experimental data on strain bursts (pop-in) during spherical indentation," *Journal of Materials Research*, vol. 35, no. 8, pp. 1028–1036, 2020.

[18] H. Vargas, J. Ramirez, and H. Arguello, "Admm-based l_1 - l_1 optimization algorithm for robust sparse channel estimation

in ofdm systems," *Signal Processing*, vol. 167, Article ID 107296, 2020.

[19] T. Hu, X. Lin, X. Wang, and P. Du, "Supervised learning algorithm based on spike optimization mechanism for multilayer spiking neural networks," *International Journal of Machine Learning and Cybernetics*, vol. 13, no. 7, pp. 1981–1995, 2022.

[20] G. Dhiman, V. Kumar, A. Kaur, and A. Sharma, "Don: deep learning and optimization-based framework for detection of novel coronavirus disease using x-ray images," *Interdisciplinary Sciences: Computational Life Sciences*, vol. 13, 2021.

[21] J. Jayakumar, S. Nagaraj, P. Chacko, and P. Ajay, "Conceptual implementation of artificial intelligent based E-mobility controller in smart city environment," *Wireless Communications and Mobile Computing*, vol. 2021, Article ID 5325116, 8 pages, 2021.

[22] X. Liu, C. Ma, and C. Yang, "Power station flue gas desulfurization system based on automatic online monitoring platform," *Journal of Digital Information Management*, vol. 13, pp. 480–488, 2015.

[23] R. Huang and X. Yang, "The application of TiO2 and noble metal nanomaterials in tele materials," *Journal of Ceramic Processing Research*, vol. 23, no. 2, pp. 213–220, 2022.

[24] Q. Zhang, "Relay vibration protection simulation experimental platform based on signal reconstruction of MATLAB software," *Nonlinear Engineering*, vol. 10, no. 1, pp. 461–468, 2021.